J. Pharm. Pharmacol. 1997, 49: 305–309
Received September 4, 1996
Accepted November 7, 1996

Estimation of the Chemosensitizing Activity of Modulators of Multi-drug Resistance via Combined Simultaneous Analysis of Sigmoidal Dose–Response Curves

GERHARD ECKER, PETER CHIBA* AND KLAUS-JÜRGEN SCHAPER†

*Institute of Pharmaceutical Chemistry and *Institute of Medical Chemistry, University of Vienna, Währingerstrasse 10, A-1090 Wien, Austria, and †Medicinal-Pharmaceutical Chemistry, Borstel Research Center, Parkallee 1-40, D-23845 Borstel, Germany*

Abstract

The potency of modulators which re-establish sensitivity of resistant tumour cells to cytotoxic drugs is not usually described by ED50 values, even though such values are needed for comparison of modulator activity.

Various methods are reported for the determination of ED50 values of propafenone-type modulators of multi-drug resistance in cytotoxicity assays. Best results were obtained by using a combined simultaneous analysis of dose–response curve families. This approach enables calculation of statistically highly significant ED50 values without any data reduction directly from the original data points obtained in daunomycin cytotoxicity assays.

The method also enables extrapolation of the ED50 values of compounds with low activity or poor solubility, or both.

Cellular resistance to a broad spectrum of cytostatic drugs is an increasing problem in cancer therapy. The phenomenon of multi-drug resistance (MDR) confers resistance to a large variety of structurally and functionally diverse drugs, such as anthracyclines, epipodophyllotoxins, actinomycin D, vinca alkaloids, colchicine and taxol (Bradley et al 1988). The cross-resistance profile is usually accompanied by a reduction in drug accumulation in resistant cells and it has been shown that this decrease in intracellular drug levels is often mediated by the expression of P-glycoprotein. This trans-membrane protein functions as an ATP-driven efflux pump for a wide variety of cytotoxic drugs (Horio et al 1988). Several substances have been identified which are able to re-establish sensitivity of resistant tumour cells to cytotoxic drugs in-vitro (Ecker & Chiba 1995).

Different approaches are used to define modulatory potency. Potency is not usually described by ED50 values; most authors determine the MDR ratio, or MDR-fold reversion, which is expressed as the ratio of the ED50 value of a toxin in the absence of modifier and the ED50 value of the toxin in the presence of a fixed concentration of modulator (Ford et al 1989; Dhainaut et al 1992). A comparison of modulator potencies is attempted under the assumption that modulator efficacies are equal. Some papers give changes in the ED10 or ED50 values of modifiers at fixed toxin concentrations (Dodic et al 1995). For rational modifier design, which requires the search for quantitative structure–activity relationships, there is, however, a need for precise and comparable modifier activity data, e.g. ED50 values, for modulating activity. In this paper, various methods based on simultaneous analysis of dose–response curve families are reported for the determination of modulator ED50 values using cytotoxicity assay data.

Correspondence: K.-J. Schaper, Medicinal-Pharmaceutical Chemistry, Borstel Research Center, Parkallee 1-40, D-23845 Borstel, Germany.

Materials and Methods

Chemistry

Compounds **1a-k** and **2a-e**, the chemical structures of which are given in Fig. 1, were prepared as described elsewhere (Ecker et al 1994, 1995, 1996; Chiba et al 1996).

Cell lines and culture conditions

The CCRF-CEM T lymphoblast cell line and the resistant line were obtained as described previously (Chiba et al 1996). Cells were kept in RPMI1640 medium supplemented with 10% foetal calf serum under standard culture conditions. The resistant CCRF vcr 100 cell line was kept in the continuous presence of 100 ng mL^{-1} vincristine. The selecting agent was washed out at least 1 week before the experiments. The cell line used in our studies was selected in the presence of increasing doses of vincristine without prior mutation. This cell line has been chosen on basis of distinct P-glycoprotein expression and does not show the mutation at codon 185. In addition, no significant contribution of other factors to MDR could be observed (unpublished data).

Cell cytotoxicity assay

The assay is dependent on the cellular reduction of MTT (3-(4,5-dimethylthiazol-2-yl)-2,5-diphenyltetrazolium bromide; Sigma, St Louis, MO) to water-insoluble formazan in the mitochondria of viable cells. The assays were performed in 96-well plates essentially as described by Mosmann (1983), with the exception that water-insoluble formazan granules were dissolved in 0·04 M HCl in 2-propanol. The absorbance was read spectrophotometrically using an EL311 Biotek microtiter plate reader (Biotek Instruments, Highland Park, VT).

The chemosensitizing effect of the propafenone-type modulators relative to daunomycin was determined using CCRF-CEM vcr 100 cells. One independent experiment represents the evaluation of the toxicity of daunomycin in CCRF-CEM vcr

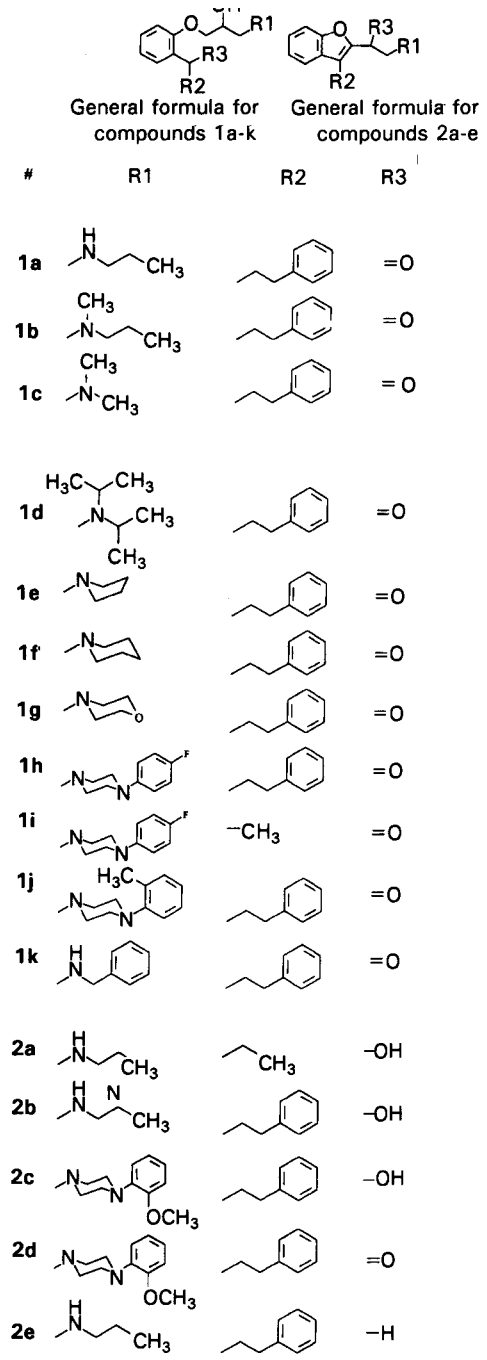

FIG. 1. The chemical structures of the compounds investigated.

100 cells in the presence of six different concentrations of a modifier. Each experiment also includes the measurement of a dose–response curve for daunomycin without modifier (VCR-control) and of one curve of the non-resistant, wild-type CCRF-CEM line (WT-control). Six different concentrations of toxin were usually used for each dose–response curve (Fig. 2).

In a first step, these experiments were analysed conventionally by fitting each dose–response curve of daunomycin according to equation 1:

$$\%S = 100 - 100[T]^a/(ED50_T{}^a + [T]^a) \quad (1)$$

where %S is the percentage survival, [T] the concentration of the toxin daunomycin, $ED50_T$ the ED50 value of daunomycin for a given concentration of modulator and a the Hill coefficient of daunomycin-toxicity curves. This model leads to eight ED50 values for daunomycin and the corresponding Hill coefficients. A plot of $ED50_T$ values against log (modulator concentration) leads to a sigmoidal dose–response curve which enables estimation of the ED50 value of the respective modulator according to equations 2a and 2b. To describe this dose–response curve a Minmax function was used with the minimum effect (MIN) being expressed as the ED50 value of toxin in the absence of modulator and the maximum possible effect (MAX) corresponding to complete reversion, represented by the ED50 value of toxin in the parental CCRF-CEM line (Fig. 3):

$$ED50_T = MIN - (MIN - MAX)\,[M]^b/(ED50_M{}^b + [M]^b) \quad (2a)$$

$$ED50_T = ED50_{VCR} - (ED50_{VCR} - ED50_{WT})\,[M]^b/(ED50_M{}^b + [M]^b) \quad (2b)$$

$ED50_T$ represents the ED50 value of daunomycin observed in the presence of a given concentration of modulator, $ED50_{VCR}$ and $ED50_{WT}$ are the ED50 values of daunomycin for the resistant CCRF-CEM vcr 100 control and the sensitive CCRF-CEM wild-type control (to generate more precise results these values are used individually for each experiment), [M] is the concentration of modulator, $ED50_M$ is the ED50 value of the modulator and b represents the Hill coefficient of the dose–response curve of the modulator. ED50 values of the modulators are listed in Table 1 (column-named single fit).

According to De Lean et al (1978), efficient data analysis should involve simultaneous description of all dose–response curves, rather than fitting them individually. A simultaneous analysis of daunomycin toxicity curve families was, therefore, performed according to equation 1 using a previously described algorithm for non-linear least squares fit (Schaper et al

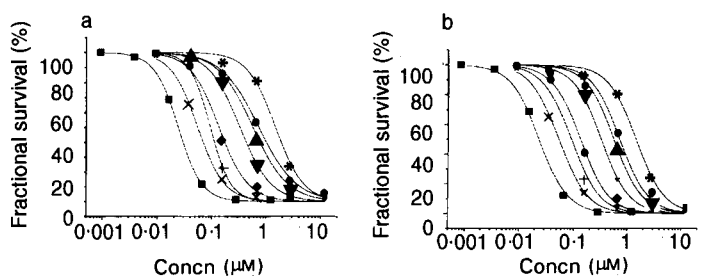

FIG. 2. Toxicity of daunomycin to CCRF-CEM vcr 100 cells in the presence of various concentrations of **1a**: (■) wild type CCRF-CEM control, (●) 0·31 μM, (▲) 0·63 μM, (▼) 1·25 μM, (◆) 2·5 μM, (+) 5·0 μM, (×) 10·0 μM, and (*) CCRF-CEM vcr 100 control: a. single fit of each dose–response curve, b. simultaneous fit of all dose–response curves.

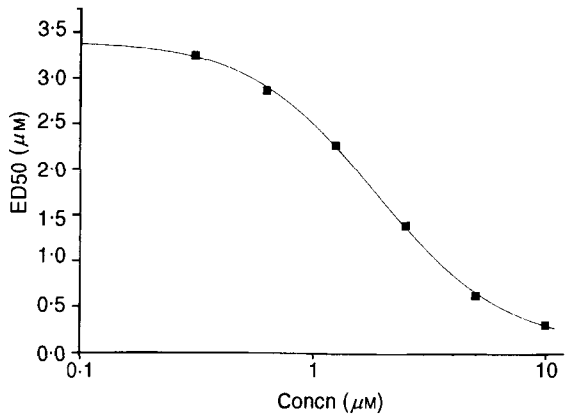

FIG. 3. Modulatory activity of compound **1g** obtained using daunomycin cytotoxicity assay. The dose–response curve was calculated using the single–fit procedure (ED50 = 1·85 μM).

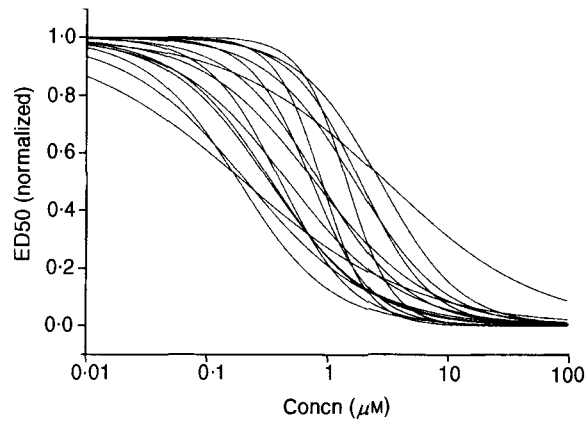

FIG. 4. Dose–response curves of all modulators tested. Potency for all modulators was normalized to values 0–1 using the minmax function.

1995). This analysis leads to eight $ED50_T$ values for daunomycin and only one Hill coefficient, a, for each cytotoxicity experiment with one modulator tested at eight concentrations (Fig. 2b). Using this procedure for estimation of $ED50_T$ values, modulator $ED50_M$ values were subsequently derived from these $ED50_T$ values by use of equation 2. The $ED50_M$ values are also presented in Table 1 (column-simultaneous toxin fit).

According to Schaper et al (1995) it is possible to analyse the dose–response curves of different drugs simultaneously under the assumption that all derivatives have the same mechanism of action within a given test model and, therefore, also have the same Hill coefficient. As previously demonstrated, this is so for the homologous series of propafenone-type MDR-modulators presented in this investigation (Chiba et al 1996). Further evidence is presented in Fig. 4, which shows that most of the dose–response curves of modulators obtained by plotting $ED50_T$ values (estimated by the simultaneous toxin fit procedure) are almost parallel. Curves showing different Hill coefficients, b, were derived from incomplete data. Thus, dose–response curves observed for all modulators were simultaneously analysed according to equation 2. This approach, which consists of two steps (step 1: simultaneous fit of all toxin dose–response curves (equation 1) leading to a set of $ED50_T$ values; step 2: simultaneous and independent fit of all modulator dose–response curves (equation 2) using $ED50_T$ values of step 1) leads to a further set of $ED50_M$ values of modulators (Table 1, column-double fit) and only one Hill coefficient, b, for all modulator dose–response curves.

By estimating eight $ED50_T$ values from 48 experimentally determined data points followed by estimation of one $ED50_M$ value the simultaneous toxin-fit approach results in an enormous concentration of information content within the available data. We therefore combined the two independent simultaneous-fit procedures (double-fit approach) by use of equation 3. This new approach enables determination of $ED50_M$ values of modulators directly from the original daunomycin toxicity

Table 1. The pharmacological activity of [ED50 (μM)] compounds **1a-k** and **2a-e**.

Compound	Single fit	Simultaneous toxin fit	Double fit	Combined simultaneous fit	Efflux
1a	0·33 ± 0·08	0·33 ± 0·08	0·37 ± 0·14	0·34 ± 0·08	3·55
1b	0·22 ± 0·21	0·21 ± 0·21	0·29 ± 0·22	0·37 ± 0·08	1·36
1c*	0·11 ± 1·85	0·20 ± 2·41	0·93 ± 0·91	0·81 ± 0·24	7·12
1d	0·81 ± 0·31	0·74 ± 0·28	0·69 ± 0·30	0·29 ± 0·07	0·61
1e*	1·46 ± 0·69	1·43 ± 0·73	0·85 ± 0·97	0·52 ± 0·16	2·55
1f*	0·51 ± 0·17	0·47 ± 1·85	0·23 ± 0·54	0·21 ± 0·06	1·65
1g	1·85 ± 0·08	1·85 ± 0·05	1·87 ± 0·27	1·43 ± 0·38	13·56
1h	0·18 ± 0·03	0·34 ± 0·03	0·29 ± 0·13	0·18 ± 0·03	0·16
1i*	0·74 ± 4·09	0·78 ± 4·09	1·21 ± 0·76	0·89 ± 0·25	8·61
1j	0·18 ± 0·03	0·18 ± 0·03	0·08 ± 0·05	0·03 ± 0·01	0·06
1k	0·98 ± 0·26	0·89 ± 0·26	0·39 ± 1·18	0·19 ± 0·05	0·41
2a	2·60 ± 3·80	2·96 ± 3·83	2·35 ± 1·85	4·19 ± 1·61	69·60
2b*	1·85 ± 0·13	1·67 ± 0·13	1·80 ± 1·10	1·59 ± 0·52	13·61
2c	0·42 ± 0·05	0·41 ± 0·05	0·40 ± 0·13	0·21 ± 0·05	0·46
2d*	2·68 ± 2·62	2·66 ± 2·62	2·76 ± 1·24	2·02 ± 0·58	4·96
2e	0·82 ± 0·49	0·86 ± 0·49	1·26 ± 1·01	0·87 ± 0·24	2·90

Values are ED50 values (± 95% confidence interval) of all modulators obtained in the MTT assay by various fit procedures. *ED50 values obtained using only three different modulator concentrations. ED50 values obtained using Rh-123 efflux represent the mean of at least two independently performed experiments. Standard deviations were usually below 15%.

data sets

$$\%S = 100 - 100[T]^a/\{[ED50_{VCR} - (ED50_{VCR} - ED50_{WT})\,[M]^b/(ED50_M{}^b + [M]^b)]^a + [T]^a\} \quad (3)$$

The abbreviations used are the same as before. $ED50_M$ values of modulators calculated by this approach are listed in Table 1 (column-combined simultaneous fit). The combined fit algorithm (equation 3) used for the simultaneous calculation of several $ED50_M$ values is a slight modification of the algorithm described recently (Schaper et al 1995). The previous number of two independent variables is increased by 1 (i.e. [M]). The Hill coefficient, a, was obtained from simultaneous analysis of all toxin dose–response curves using equation 1.

Analysis of incomplete data sets

For compounds with low activity or poor solubility, or both, it is sometimes not possible to obtain complete dose–response curves. In this circumstance the simultaneous analysis of dose–response curve families of a homologous series of drugs enables calculation of statistically significant ED50 values of these substances (Schaper et al 1995). To check the accuracy of this approach, we included a series of cytotoxicity assays performed using only three different concentrations of modifier (indicated with an asterisk in Table 1).

Rhodamine-123 efflux studies

The rhodamine-123 assay is a well documented direct and extremely reproducible functional assay for measuring P-glycoprotein-dependent efflux (Drach et al 1992). ED50 values of modulators obtained by this method were, therefore, used as reference values. We measured the ability of several propafenone analogues to inhibit P-glycoprotein-mediated rhodamine-123 efflux in resistant CCRF-CEM vcr 100 cells.

Rhodamine efflux studies were performed by analogy with previously published methods (Chiba et al 1996). Cells were pelleted, the supernatant was removed by suction and the cells were resuspended at a density of 1×10^6 mL^{-1} in RPMI1640 medium containing rhodamine-123 (Sigma) at a final concentration of 0·2 μg mL^{-1}. Cell suspensions were incubated at 37°C for 15 min. Tubes were chilled on ice and pelleted at 500 *g* in an Eppendorf 5403 centrifuge (Eppendorf, Germany). Supernatant was removed and the cell pellet was resuspended in medium which was pre-warmed to 37°C and contained either no modulator or chemosensitizer at various concentrations ranging from 16 nM to 500 μM, depending on the solubility and expected potency of the modifier. Eight concentrations (serial dilution 1 : 2·5) were tested for each modulator. After 30, 60, 90 and 120 s samples of the incubation mixture were transferred to tubes containing an equal volume of ice-cold stop solution (RPMI1640 medium containing verapamil at a final concentration of 10 μg mL^{-1}). Zero time points were obtained by immediately pipetting rhodamine-123 pre-loaded cells into ice-cold stop solution. Non-P-glycoprotein-expressing parental CCRF-CEM cells were used as controls for simple plasma-membrane diffusion, whereby initial rhodamine-123 fluorescence levels were adjusted to be equal to initial levels observed in resistant cells. Samples drawn at the respective time-points were kept in an ice-water bath and measured within 1 h on a Becton Dickinson Facscalibur flow cytometer (Becton Dickinson, Vienna, Austria). Viable cells were gated on the basis of forward and side scatter. Five thousand gated events were accumulated for the determination of mean fluorescence values. The time-dependent decrease in mean fluorescence values was linear for at least 2 min and was expressed as the percentage of the values of the corresponding zero time points, to enable comparison of independent experiments.

The time-dependent linear decrease in mean fluorescence in the presence of various concentrations of modifier was estimated and the initial efflux rates were calculated by linear regression analysis. Correction for simple diffusion was achieved by subtracting the efflux rates observed in the parental, non-P-glycoprotein-expressing line. ED50 values of all modifiers were determined from dose–response curves of initial efflux rates against modifier concentration and are given in Table 1. Data points from at least two independently performed experiments were fitted according to equation 4, where y is the initial rate of efflux determined as a function of modifier concentration, c, y_i is the initial efflux rate in absence of modulator and ME is the modulatory efficacy:

$$y = y_i - ME \cdot c/(ED50 + c) \quad (4)$$

Fit procedures

The fit of dose–response equations to single curves was performed using the software package Microcal Origin, installed on an IBM-compatible computer (468 DX2). The simultaneous analysis of dose–response curves was performed on a personal computer using an in-house software package (K.-J. Schaper, Borstel, Germany).

Results and Discussion

To prove the accuracy of our new method, we estimated the MDR-modulating activity of a series of propafenone analogues using an MTT-based cytotoxicity assay. The rhodamine-123 efflux assay, which is a highly reproducible functional assay for measuring P-glycoprotein-dependent efflux, was used as a reference method. As previously demonstrated, the CCRF-CEM vcr cell lines exhibit the MDR phenotype owing to overexpression of P-glycoprotein. No other reasons for resistance could be detected. Thus, cytotoxicity data obtained with CCRF-CEM vcr cells should show a stringent correlation with rhodamine-123 efflux data.

A gradual improvement in the correlation between MTT-assay and the efflux experiments can be observed by stepwise inclusion of data points in the simultaneous fitting procedure: (a) fit of dose–response curves of toxins at individual modifier concentrations (single fit); (b) simultaneous fit of eight dose–response curves for toxin at eight different concentrations of one modulator (simultaneous toxin fit); (c) simultaneous fit of all toxin curves and simultaneous (but independent) fit of all modulator dose–response curves (double fit); and (d) combined simultaneous fit of original cytotoxicity data points for all modulators (combined simultaneous fit). $ED50_M$ values obtained by fit procedures a-d and analogous values obtained in rhodamine-123 efflux studies were compared by linear regression analysis of the corresponding log (1/ED50) values. In this analysis the compounds with incomplete dose–response curves were also included. The best correlation was obtained by using the combined simultaneous fit analysis for data pro-

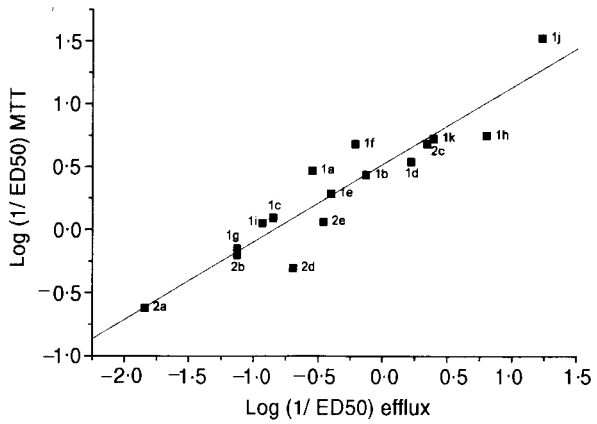

FIG. 5. Correlation of modulatory potencies (expressed as log (1/ED50) values; ED50 in μM) obtained in daunomycin cytotoxicity assays (MTT assay; values obtained using combined simultaneous-fit procedure) and rhodamine-123 efflux studies ($r = 0{\cdot}93$).

cessing ($r = 0{\cdot}93$, $n = 16$; Fig. 5). Regression analysis of the efflux data with the $ED50_M$ values obtained by the double-fit, simultaneous-toxin-fit or single-fit procedure resulted only in r values of 0·84, 0·63 and 0·58, respectively. Thus, using a combined simultaneous analysis of dose–response curve families of homologous drugs for analysis of cytotoxicity assays leads to highly significant ED50 values for modulators, which should enable the derivation of more informative and significant equations for quantitative structure–activity relationships.

The analysis of incomplete data sets by use of the combined simultaneous fit-curve algorithm shows that this is also a versatile method for analysing the activity of only slightly active or poorly soluble compounds (compounds marked with an asterisk in Table 1).

Conclusions

The combined simultaneous analysis of dose–response curve families of homologous drug series is a powerful method for the estimation of the pharmacological activity of MDR-modulators using cytotoxicity assays. This method enables the calculation of statistically highly significant Hill coefficients and ED50 values. ED50 values can, furthermore, be estimated for compounds which are poorly soluble or only slightly active, or both, with incomplete data sets. Each additional data set contributes to a statistically more precise estimation of variables (i.e. Hill coefficients) that are equal for all modulators. This information is lost when using individual fit procedures. By using a combined simultaneous-fit procedure, this information is conserved and can be used to facilitate the derivation of more informative and significant equations for quantitative structure–activity relationships.

Acknowledgements

P. Chiba thanks the Jubiläumsfond of the Austrian National Bank for financial support (grant number 4728). G. Ecker thanks the University of Vienna for financial support.

References

Bradley, G., Juranka, P. F., Ling, V. (1988) Mechanism of multidrug resistance. Biochim. Biophys. Acta 948: 87–128

Chiba, P., Ecker, G., Schmid, D., Drach, J., Tell, B., Goldenberg, S., Gekeler, V. (1996) Structural requirements for activity of propafenone type modulators in PGP-mediated multidrug resistance. Mol. Pharmacol. 49: 1122–1130

De Lean, A., Munson, P. J., Rodbard, D. (1978) Simultaneous analysis of families of sigmoidal curves: application to bioassay, radioligand assay, and physiological dose–response curves. Am. J. Physiol. 235: E97–E102

Dhainaut, A., Regnier, G., Atassi, G., Pierre, A., Leonce, S., Kraus-Berthier, L., Prost, J.-F. (1992) New triazine derivatives as potent modulators of multidrug resistance. J. Med. Chem. 35: 2481–2496

Dodic, N., Dumaitre, B., Daugan, A., Pianetti, P. (1995) Synthesis and activity against multidrug resistance in Chinese hamster ovary cells of new acridone-4-carboxamides. J. Med. Chem. 38: 2418–2426

Drach, D., Zhao, S., Drach, J., Mahadevia, R., Gattringer, C., Huber, H., Andreeff, M. (1992) Subpopulations of normal peripheral blood and bone marrow cells express a functional multidrug resistant phenotype. Blood 80: 2729–2734

Ecker, G., Chiba, P. (1995) Structure–activity-relationship studies on modulators of the multidrug transporter P-glycoprotein–an overview. Wien. Klin. Wochenschr. 107: 681–686

Ecker, G., Fleischhacker, W., Noe, C. R. (1994) New benzofuran-type antiarrhythmic compounds related to propafenone. Heterocycles 38: 1247–1256

Ecker, G., Fleischhacker, W., Helml, T., Noe, C. R., Studenik, C., Schade, B., Heistracher, P. (1995) Synthesis and pharmacodynamic activity of 2-(3-(2-phenylethyl)benzofuran-2-yl)-*N*-propylethanamine. Arch. Pharm. 328: 343–348

Ecker, G., Chiba, P., Hitzler, M., Schmid, D., Visser, K., Cordes, H. P., Csöllei, J., Seydel, J. K., Schaper, K.-J. (1996) Structure–activity relationship studies on benzofuran analogs of propafenone-type modulators of tumor cell multidrug resistance. J. Med. Chem. 39: 4767–4774

Ford, J. M., Prozialeck, W. C., Hait, W. N. (1989) Structural features determining activity of phenothiazines and related drugs for inhibition of cell growth and reversal of multidrug resistance. Mol. Pharmacol. 35: 105–115

Horio, M., Gottesman, M. M., Pastan, I. (1988) ATP-dependent transport of vinblastine in vesicles from human multidrug-resistant cells. Proc. Natl Acad. Sci. USA 85: 3580–3584

Mosmann, T. (1983) Rapid colorimetric assay for cellular growth and survival: application to proliferation and cytotoxicity assays. J. Immunol. Meth. 65: 55–63

Schaper, K.-J., Emig, P., Engel, J., Fleischhauer, I., Kutscher, B., Rosado Samitier, M. L., Lopez Rodriguez, M. L. (1995) Dose response relationships, biotest intercorrelations, QSAR and the saving of animal experiments. In: Sanz, F., Giraldo, J., Manaut, F. (eds) QSAR and Molecular Modelling: Concepts, Computational Tools and Biological Applications. J. R. Prous Science Publishers, Barcelona, pp 73–76

J. Pharm. Pharmacol. 1997, 49: 310–314
Received July 15, 1996
Accepted October 22, 1996

Age-related Changes in [^{3}H]Nimodipine and [^{3}H]Rolipram Binding in the Rat Brain

T. ARAKI, H. KATO, K. SHUTO* AND Y. ITOYAMA

*Department of Neurology, Tohoku University School of Medicine, Sendai, and *Pharmacological Research Laboratory, Research Laboratories, Tokyo Tanabe Co. Ltd, Tokyo, Japan*

Abstract

Ageing is associated with changes in neurotransmission which might be correlated with abnormal calcium metabolism. Because there is evidence that nimodipine can enhance the learning abilities of ageing animals and rolipram can enhance the excitability of neurons, providing a functional basis for cognition-enhancing activity, age-related alterations in the binding of voltage-dependent L-type calcium channels and calcium/calmodulin-independent cyclic adenosine monophosphate-selective phosphodiesterase (cyclic-AMP PDE) were studied in 3-week- and 6-, 12-, 18- and 24-month-old Fisher 344 rats by use of receptor autoradiography.

[^{3}H]Nimodipine and [^{3}H]rolipram were used to label the voltage-dependent L-type calcium channels and calcium/calmodulin-independent cyclic-AMP PDE, respectively. [^{3}H]Nimodipine binding showed no obvious change in all brain areas of 12- and 18-month-old rats, as compared with 6-month-old animals. In 24-month-old rats, however, [^{3}H]nimodipine binding increased significantly in the striatum and hippocampal CA3 sector. In contrast, [^{3}H]rolipram binding showed no significant change in most brain areas during ageing, except for a transient change only in the hippocampal CA1 sector of 12-month-old animals. [^{3}H]Nimodipine and [^{3}H]rolipram binding showed a significant increase in some brain areas of 3-week-old rats compared with 6-month-old animals.

The results indicate that in rats voltage-dependent L-type calcium channels are more susceptible to ageing processes than calcium/calmodulin-independent cyclic-AMP PDE. Our data also demonstrate that voltage-dependent L-type calcium channels and calcium/calmodulin-independent cyclic-AMP PDE might play roles in developmental processes. These findings might help further elucidation of the relationship between age-related neurological deficits and behavioural pharmacology including cognitive function.

Nimodipine is a potent voltage-dependent L-type calcium channel antagonist which has a high affinity for the central nervous system and passes the blood-brain barrier rapidly (Scriabine et al 1989). Several lines of evidence have demonstrated that nimodipine can enhance the learning abilities of ageing rabbits, rats and monkeys (Deyo et al 1989; Sandin et al 1990; Straube et al 1990; Levere & Walker 1991). This drug has also been reported to be effective for the treatment of age-related disorders such as senile dementia (Tollefson 1990). There has, furthermore, been growing interest in the application of nimodipine as a protective agent against ischaemic brain damage (Uematsu et al 1991; Roda et al 1995). From these observations it is conceivable that nimodipine might have a role in the treatment of age-related neurological deficits and cognitive dysfunction. Little is, however, known about changes of [^{3}H]nimodipine binding in the ageing process.

Rolipram, known to be an antidepressant, inhibits a calcium/calmodulin-independent cyclic adenosine monophosphate-selective phosphodiesterase (cyclic-AMP PDE) isozyme (Kariya & Dage 1988), leading to an increase in brain cyclic-AMP levels (Schneider 1984). Regional distributions for [^{3}H]rolipram binding sites have been quantified and visualized in the brain by receptor autoradiography (Kaulen et al 1989). A recent study suggests that the PDE inhibitor denbufylline can enhance the excitability of neurons, providing a functional basis for cognition-enhancing activity (Nicholson et al 1991). The calcium/calmodulin-independent cyclic-AMP PDE might therefore, play a role in modulation of brain function, although the role of the cyclic-AMP PDE in ageing process is not fully understood.

In this study we have, therefore, used receptor autoradiography to investigate age-related changes in voltage-dependent L-type calcium channels and calcium/calmodulin-independent cyclic-AMP PDE in aged rat brain.

Correspondence: T. Araki, Department of Neurology, Tohoku University School of Medicine, 1-1 Seiryo-machi, Aoba-ku, Sendai 980, Japan.

Materials and Methods

Subjects

Male Fisher 344 rats, 3 weeks and 6, 12, 18 and 24 months old, were used. The animals were lightly anaesthetized with ether and then killed by decapitation. The brains were removed immediately, frozen in powdered dry ice, and stored at −80°C until assay. Sagittal sections 12 μm thick were cut on a cryostat and thaw-mounted on to gelatin-coated cover slides. Adjacent sections stained with cresyl violet were examined with a light-microscope. Each group contained five to seven rats.

Receptor autoradiography

[^{3}H]Nimodipine binding. Autoradiographic localization of voltage-dependent L-type calcium channels was detected using [^{3}H]nimodipine by the methods of Bellemann et al (1983) with minor modifications. Brain sections were pre-incubated for 30 min at room temperature in 50 mM Tris-HCl buffer (pH 7·4) containing 150 mM NaCl and 1 mM $CaCl_2$. The sections were then incubated with 1·5 nM [^{3}H]nimodipine (specific activity, 152 Ci mmol^{-1} (NEN)) in the same buffer

for 60 min at room temperature. After incubation, the sections were washed twice for 10 min at 4°C in fresh buffer. Non-specific binding was determined by use of 15 μM nimodipine (Sigma) under the same experimental conditions.

[^{3}H]Rolipram binding. Autoradiographic distribution of calcium/calmodulin-independent cyclic-AMP PDE inhibitor binding sites was detected using [^{3}H]rolipram according to the method of Kaulen et al (1989) with minor modifications (Araki et al 1992). Brain sections were incubated for 60 min at 0°C with 5 nM [^{3}H]rolipram (specific activity 60 Ci mmol^{-1}; Amersham) in 150 mM phosphate buffer (pH 7·4) containing 2 mM $MgCl_2$ and 100 μM dithiothreitol. After incubation the sections were washed twice with fresh buffer for 30 s at 0°C and briefly rinsed in ice-cold distilled water. Non-specific binding was determined using 1 μM rolipram (Meiji Seika Co. Ltd, Yokohama, Japan) under the same experimental conditions.

Data analysis

The sections were quickly dried under a cold air stream and were exposed to Hyperfilm-^{3}H (Amersham) for 4–6 weeks in X-ray cassettes with a set of [^{3}H]microscales (Amersham). The optical density of the brain areas was measured with a computer-controlled image analyser, as described previously (Araki et al 1995). Binding assays were performed in duplicate under subdued lighting. Values were expressed as means ± s.d. Statistical significance was determined by analysis of variance then Dunnett's multiple comparison test.

Results

Regional age-related alterations of [^{3}H]nimodipine and [^{3}H]rolipram binding are summarized in Tables 1 and 2. Representative autoradiograms of this binding are shown in Fig. 1.

Receptor autoradiography

[^{3}H]Nimodipine binding. The localization of [^{3}H]nimodipine binding was relatively heterogeneous throughout the brain. In adult (6-month-old) rats the highest [^{3}H]nimodipine binding was evident in the hippocampus, followed by the neocortex, thalamus, cerebellum and striatum. Other regions showed relatively low [^{3}H]nimodipine binding. In immature (3-week-old) rats a significant increase in [^{3}H]nimodipine binding was observed in the striatum and hippocampal CA3 sector and thalamus, compared with those regions in the adult animals. Other regions showed no significant change in [^{3}H]nimodipine binding. [^{3}H]nimodipine binding, on the other hand, was not significantly different in the brains of 12- and 18-month-old rats. In 24-month-old rats, however, a significant increase in [^{3}H]nimodipine binding was found in the striatum and hippocampal CA3 sector. Other regions showed no significant alteration in [^{3}H]nimodipine binding.

[^{3}H]Rolipram binding. In adult rats [^{3}H]rolipram binding was strikingly heterogeneous and was greatest in the hippocampus, neocortex, striatum and thalamus. Other regions had a low grain density of [^{3}H]rolipram binding. In immature rats the grain density of [^{3}H]rolipram binding was quite similar to that of the adult animals, although a significant increase in [^{3}H]rolipram binding was observed in the thalamus, substantia nigra and cerebellum of the immature rats, compared with those regions in the adult animals. Other regions showed no obvious change in [^{3}H]rolipram binding. No significant change in [^{3}H]rolipram binding was, on the other hand, seen in most brain areas in 12-, 18- and 24-month-old rats. A transient increase in [^{3}H]rolipram binding was observed only in the hippocampal CA1 sector of 12-month-old rats.

Discussion

Ageing is associated with striking changes in neurotransmission which might underlie age-dependent deficits in cognitive function and psychomotor performance (Bartus et al 1982; Joseph et al 1983). These deficits might, at least in part, be correlated with abnormal calcium metabolism. For example, calcium-dependent acetylcholine release is reduced in the brain of aged mice (Gibson & Peterson 1981) and perturbations in normal calcium metabolism have been correlated with learning and memory deficits in aged rabbits (Deyo et al 1989). Several studies have, furthermore, reported that brain ageing is accompanied by a reduction in calcium uptake (Gibson & Peterson 1987; Martinez et al 1987). Thus age-related changes in calcium metabolism might affect neuronal functions such as neurotransmitter release and neurotransmission.

In this study, no significant increase in [^{3}H]nimodipine binding was observed in any brain areas of 12- and 18-month-

Table 1. Age-associated changes in [^{3}H]nimodipine-binding in the rat brain.

Region	Age				
	3 weeks	6 months	12 months	18 months	24 months
Frontal cortex	35 ± 6	25 ± 11	24 ± 6	25 ± 10	37 ± 6
Parietal cortex	32 ± 6	30 ± 15	31 ± 7	28 ± 17	35 ± 7
Striatum	41 ± 8*	21 ± 10	25 ± 5	24 ± 10	43 ± 9*
Hippocampus					
CA1 sector	32 ± 6	31 ± 10	35 ± 10	24 ± 14	42 ± 10
CA3 sector	60 ± 10*	40 ± 9	47 ± 6	42 ± 14	63 ± 7*
Dentate gyrus	67 ± 10	75 ± 10	85 ± 11	72 ± 17	88 ± 9
Thalamus	66 ± 13*	30 ± 10	39 ± 6	33 ± 14	46 ± 10
Substantia nigra	32 ± 18	14 ± 12	17 ± 12	14 ± 14	27 ± 10
Cerebellum	37 ± 14	24 ± 5	21 ± 7	23 ± 9	22 ± 10

Optical density was converted to fmol (mg tissue)$^{-1}$ by use of [^{3}H]microscales. Values are expressed as means ± s.d. *$P < 0.01$ compared with 6-month-old group (Dunnett's multiple range test; n = 5–7).

Table 2. Age-associated changes in [^{3}H]rolipram-binding in the rat brain.

Region	Age				
	3 weeks	6 months	12 months	18 months	24 months
Frontal cortex	112 ± 20	102 ± 19	119 ± 16	91 ± 15	91 ± 15
Parietal cortex	100 ± 17	85 ± 14	106 ± 20	97 ± 17	90 ± 14
Striatum	73 ± 13	74 ± 81	82 ± 12	69 ± 13	77 ± 12
Hippocampus					
CA1 sector	104 ± 22	127 ± 15	156 ± 19*	148 ± 19	142 ± 20
CA3 sector	123 ± 23	123 ± 12	145 ± 32	129 ± 20	123 ± 16
Dentate gyrus	95 ± 14	89 ± 18	95 ± 18	85 ± 5	86 ± 15
Thalamus	138 ± 22†	87 ± 12	95 ± 16	82 ± 13	87 ± 18
Substantia nigra	64 ± 16†	43 ± 9	45 ± 8	41 ± 5	44 ± 8
Cerebellum	58 ± 12†	45 ± 7	36 ± 4	39 ± 3	37 ± 5

Optical density was converted to fmol (mg tissue)$^{-1}$ by use of [^{3}H]microscales. Values are expressed as means ± s.d. *$P < 0.05$, †$P < 0.01$ compared with 6-month-old group (Dunnett's multiple range test; n = 5–7).

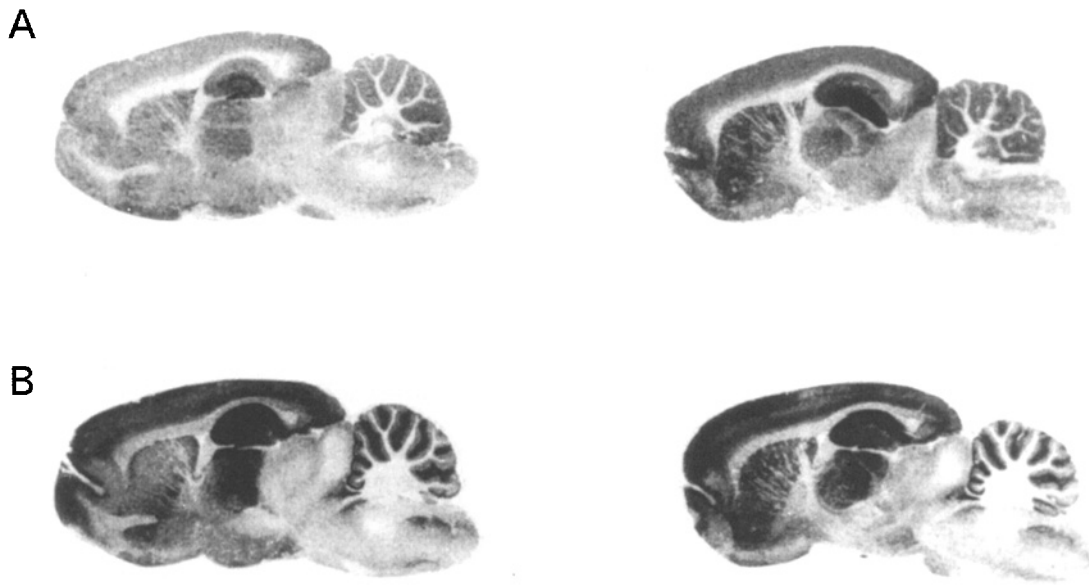

FIG. 1. Autoradiographic distribution of [^{3}H]nimodipine (A) and [^{3}H]rolipram (B) binding in the rat brain. Left: adult (6 months old) rat brain, right: aged (24 months old) rat brain. A significant increase in [^{3}H]nimodipine binding was noted in the striatum and hippocampal CA3 sector in aged rats, compared with those in adult animals (A). In contrast, no significant change in [^{3}H]rolipram binding was observed in any brain areas of aged rats (B).

old rats, as compared with those from adult animals. A significant increase in [^{3}H]nimodipine binding was, however, found in the striatum and hippocampal CA3 sector of 24-month-old rats. A previous study suggested that an age-dependent increase in [^{3}H]verapamil (a voltage-dependent calcium-channel blocker) binding was seen in the rat cortical membrane (Battaini et al 1985). Govoni et al (1985) reported, furthermore, that the number of [^{3}H]nitrendipine (a voltage-dependent calcium channel blocker) binding sites was slightly increased in the cortical membranes of 24-month-old rats. In agreement with our findings Navaratnam & Khatter (1991) have, interestingly, also observed an age-related increase in [^{3}H]nitrendipine binding in the sarcolemmal membrane. From these observations, the present study seems to suggest that calcium channels are gradually affected in ageing processes and this might lead to neurological deficits.

Several neurotransmitters are well known to stimulate the formation of cyclic-AMP by activation of adenylate cyclase (Phillis 1977). Cyclic-AMP plays a key role in expression or activation of ion channels and acetylcholine receptors (Artalejo et al 1990; Ifune & Steinbach 1990). The cyclic-AMP cascade, including adenylate cyclase, is involved in learning, short-term memory and synaptic plasticity (Buxbaum & Dudai 1989; Zhong et al 1992) and is, therefore, implicated in ageing processes and cognitive function. Cellular cyclic nucleotide phosphodiesterases are also known to play a role in the metabolism of cyclic-AMP by determining the response intensity and duration of neurons to various neurotransmitters acting via adenylate cyclase (Kaulen et al 1989).

Rolipram is an antidepressant with calcium/calmodulin-independent specific cyclic-AMP type-IV PDE inhibitory properties, leading to increased brain cyclic-AMP levels; the

binding sites have a unique distribution showing only limited overlap with general cyclic-AMP and phosphatidylinositol-related markers (Kariya & Dage 1988; Kaulen et al 1989). These observations, therefore, imply a function for the calcium/calmodulin-independent cyclic-AMP PDE in cognitive function and ageing processes. The present study, however, showed no significant changes in [^{3}H]rolipram binding in most brain areas during ageing. These findings suggest the possibility that calcium/calmodulin-independent cyclic-AMP PDE might not play a key role in ageing processes. It is, however, now generally accepted that there are four type-IV cyclic-AMP PDE isoform families, denoted IV_A, IV_B, IV_C and IV_D (Lobban et al 1994; McPhee et al 1995), although the precise functional role of these enzymes is not fully understood. It is, therefore, necessary to investigate the regional pattern of each subtype of type-IV cyclic-AMP PDE for further understanding of age-related changes in the brain, using receptor autoradiographic and biochemical techniques.

In this study, a significant increase in [^{3}H]nimodipine binding was observed in the striatum, hippocampal CA3 sector and thalamus of 3-week-old rats as compared with those of 6-month-old rats. On the other hand, [^{3}H]rolipram binding also increased significantly in the thalamus, substantia nigra and cerebellum of 3-week-old animals. Several recent studies have demonstrated that the density of calcium channels changes during development. In isolated rat hippocampal cells the peak calcium current increases from postnatal day 12 to postnatal day 28 (Thompson & Wong 1991). In isolated rat cortical neurons, furthermore, the mean whole-cell calcium current increases with age up to approximately 3 weeks postnatal and then levels off, with a decline in adult animals (Lorenzon & Foehring 1995). Thus the present study also seems to suggest that voltage-dependent L-type calcium channels change in the brain during development. Akaike et al (1993) recently reported that rolipram can contribute to the neuronal development of PC 12 cells by increasing intracellular cyclic-AMP, which has an important role in the development of voltage-dependent calcium channels. They suggest, furthermore, that rolipram can behave like a neurotrophic factor in cultured PC12 cells. This finding is of interest in relation to developmental relationships between the voltage-dependent calcium channels and calcium/calmodulin-independent cyclic-AMP PDE. In this study, however, we have no ready precise explanation of a significant increase in [^{3}H]rolipram binding in the thalamus, substantia nigra and cerebellum of 3-week-old rats. Further studies are, therefore, needed to investigate the detailed mechanism of our findings, although the study suggests that calcium/calmodulin-independent cyclic-AMP PDE and voltage-dependent L-type calcium channels might play roles in developmental processes.

In conclusion, this study provides evidence that voltage-dependent L-type calcium channels are more susceptible to ageing processes than calcium/calmodulin-independent adenosine monophosphate-selective phosphodiesterase in rat brains. Furthermore, our results suggest that voltage-dependent L-type calcium channels and calcium/calmodulin-independent adenosine monophosphate-selective phosphodiesterase might play roles in developmental processes. These findings might help further elucidation of the relationship between age-related neurological deficits and behavioural pharmacology including cognitive function.

References

Akaike, N., Furukawa, K., Kogure, K. (1993) Rolipram enhances the development of voltage-dependent Ca^{2+} current and serotonin-induced current in rat pheochromocytoma cells. Brain Res. 620: 58–63

Araki, T., Kato, H., Kogure, K. (1992) Mapping of second messenger and rolipram receptors in mammalian brain. Brain Res. Bull. 28: 843–848

Araki, T., Kato, H., Fujiwara, T., Kogure, K., Itoyama, Y. (1995) Post-ischemic changes in [^{3}H]glycine binding in the gerbil brain after cerebral ischemia. Eur. J. Pharmacol. 278: 91–96

Artalejo, C. R., Ariano, M. J., Perlman, R. L., Fox, A. (1990) Activation of facilitation calcium channels in chromaffin cells by D_1 dopamine receptors through a cAMP/protein kinase A-dependent mechanism. Nature 348: 239–242

Bartus, R. T., Dean, R. L., Beer, B., Lippa, A. S. (1982) The cholinergic hypothesis of geriatric memory dysfunction. Science 217: 408–417

Battaini, F., Govoni, S., Rius, R. A., Trabucchi, M. (1985) Age dependent increase in [^{3}H]verapamil binding to rat cortical membrane. Neurosci. Lett. 61: 67–71

Bellemann, P., Schade, A., Towart, R. (1983) Dihydropyridine receptor in rat brain labeled with [^{3}H]nimodipine. Proc. Natl. Acad. Sci. USA 80: 2356–2360

Buxbaum, J. D., Dudai, Y. (1989) A quantitative model for the kinetics of cAMP-dependent protein kinase (type II) activity. Long-term activation of the kinase and its possible relevance to learning and memory. J. Biol. Chem. 264: 9344–9351

Deyo, R. A., Straube, K. T., Disterhoft, J. F. (1989) Nimodipine facilitates associative learning in ageing rabbits. Science 243: 809–811

Gibson, G. E., Peterson, C. D. (1981) Ageing decreases oxidative metabolism and the release and synthesis of acetylcholine. J. Neurochem. 37: 978–984

Gibson, G. E., Peterson, C. (1987) Calcium and the ageing nervous system. Neurobiol. Ageing 8: 329–334

Govoni, S., Rius, R. A., Battaini, F., Bianchi, A., Trabucchi, M. (1985) Age-related reduced affinity in [^{3}H]nitrendipine labeling of brain voltage-dependent calcium channels. Brain Res. 333: 374–377

Ifune, C. K., Steinbach, J. H. (1990) Regulation of sodium current and acetylcholine responses in PC 12 cells. Brain Res. 506: 243–248

Joseph, J. A., Bartus, R. T., Clody, D., Morgan, D., Finch, C., Beer, B., Sesack, S. (1983) Psychomotor performance in the senescent rodent: reduction of deficits via striatal dopamine receptor upregulation. Neurobiol. Ageing 4: 313–319

Kariya, T., Dage, R. C. (1988) Tissue distribution and selective inhibition of high affinity cAMP phosphodiesterase. Biochem. Pharmacol. 37: 3267–3270

Kaulen, P., Bruning, G., Schneider, H. H., Sarter, M., Baumgarten, H. G. (1989) Autoradiographic mapping of a selective cyclic adenosine monophosphate phosphodiesterase in rat brain with antidepressant [^{3}H]rolipram. Brain Res. 503: 229–245

Levere, T. E., Walker, A. (1991) Ageing and cognition: enhancement of recent memory in rats by the calcium channel blocker nimodipine. Neurobiol. Aging 13: 63–66

Lobban, M., Shakur, Y., Beattie, J., Houslay, M. D. (1994) Identification of two splice variant forms of type-IVB cyclic AMP phosphodiesterase, DPD (rPDE-IVB1) and PDE-4 (rPDE-IVB2) in brain: selective localization in membrane and cytosolic compartments and differential expression in various brain regions. Biochem. J. 304: 399–406

Lorenzon, N. M., Foehring, R. C. (1995) Characterization of pharmacologically identified voltage-gated calcium channel currents in acutely isolated rat neocortical neurons. II. Postnatal development. J. Neurophysiol. 73: 1443–1451

Martinez, A., Vitorica, J., Bogonez, E., Satrustegui, J. (1987) Differential effects of age on the pathways of calcium influx into nerve terminals. Brain Res. 435: 249–257

McPhee, I., Pooley, L., Lobban, M., Bolger, G., Houslay, M. D. (1995) Identification, characterization and regional distribution in brain of RPDE-6 (RNPDE4A5), a novel splice variant of the PDE4A cyclic AMP phosphodiesterase family. Biochem. J. 310: 965–974

Navaratnam, S., Khatter, J. C. (1991) Increased [^{3}H]nitrendipine

binding sites in rat heart during adult maturation and aging. Neuroscience 41: 593–600

Nicholson, C. D., Challiss, R. A. J., Shalid, M. (1991) Differential modulation of tissue function and therapeutic potential of selective inhibitors of cyclic nucleotides phosphodiesterase isoenzymes. Trends Pharmacol. Sci. 12: 19–27

Phillis, J. W. (1977) The role of cyclic nucleotides in the CNS. Can. J. Neurol. Sci. 2: 153–195

Roda, J. M., Carceller, F., Diez-Tejedoe, E., Avendano, C. (1995) Reduction of infarct size by intra-arterial nimodipine administered at reperfusion in a rat model of partially reversible brain focal ischemia. Stroke 26: 1888–1892

Sandin, M., Jasmin, S., Levere, T. E. (1990) Aging and cognition: facilitation of recent memory in aged nonhuman primates by nimodipine. Neurobiol. Aging 11: 567–571

Schneider, H. H. (1984) Brain cAMP response to phosphodiesterase inhibitors in rats killed by microwave irradiation or decapitation. Biochem. Pharmacol. 33: 1690–1696

Scriabine, A., Schuurman, T., Traber, J. (1989) Pharmacological basis for the use of nimodipine in central nervous system disorders. Fed. Eur. Biochem. Soc. Lett. 3: 1799–1806

Straube, K. T., Deyo, R. A., Moyer, J. R., Disterhoft, J. F. (1990) Dietary nimodipine improves associative learning in aging rabbits. Neurobiol. Aging 11: 659–661

Thompson, S. M., Wong, R. K. (1991) Development of calcium current subtypes in isolated rat hippocampal pyramidal cells. J. Physiol. 439: 671–689

Tollefson, G. D. (1990) Short-term effects of the calcium channel blocker nimodipine (Bay-e-9736) in the management of primary degenerative dementia. Biol. Psychiatry 27: 1133–1142

Uematsu, D., Araki, N., Greenberg, J. H., Sladky, J., Reivich, M. (1991) Combined therapy with MK-801 and nimodipine for protection of ischemic brain damage. Neurology 41: 88–94

Zhong, Y., Budnik, V., Wu, C. F. (1992) Synaptic plasticity in drosophila memory and hyperexcitable mutants: role of cAMP cascade. J. Neurosci. 12: 644–651

J. Pharm. Pharmacol. 1997, 49: 315–318
Received September 9, 1996
Accepted November 7, 1996

Anticholinergic Activity in Mice and Receptor-binding Properties in Rats of a Series of Synthetic Tropane Derivatives

Z. G. GAO*, W. Y. CUI, B. Y. LIU, C. G. LIU AND L. WANG

Institute of Pharmacology and Toxicology, 27 Taiping Road, Beijing 100850, China

Abstract

A tropane ester, three tropane ethers, atropine and mecamylamine were compared in mice for their anti-muscarinic and anti-nicotinic activity against arecoline-induced tremor and nicotine-induced convulsions, respectively. Their receptor-binding characteristics were studied in neuronal membranes prepared from rat cerebral cortex.

The results showed that the tropane ester, 2α*R*-tropanyl benzylate, was more potent than atropine in its anti-muscarinic activity, but the anti-muscarinic activity of the tropane ethers, 2α-(2′,2′-diphenyl-2′-hydroxyethoxy)tropane (α-DPT) and its two isomers (1*R*,2α*R*- and 1*S*,2α*S*-) were less potent than that of atropine. In contrast with their anti-muscarinic potency, 2α*R*-tropanyl benzylate and the three tropane ethers were equipotent in their anti-nicotinic activities. The order of potencies of these compounds to displace the binding of [^{3}H]quinuclidinyl benzylate to brain membranes was similar to that of their anti-muscarinic potencies. The binding of [^{3}H]nicotine to nicotinic receptors from brain was not inhibited by these compounds.

Analyses of structure–activity relationships of these compounds suggested that it is the ester groups that determine the anti-muscarinic potencies of 2α*R*-tropanyl benzylate; their anti-nicotinic activities were independent of the structural changes and of the anti-muscarinic activities of these compounds.

Relationships between the stereochemistry and the biological activity of anticholinergic compounds are well known (Hoyer 1986; Waelbroeck et al 1989; Noronha-blob & Kachur 1991). In the specific case of aminoalcohol esters, the importance of stereochemistry is shown by the fact that (−)-3-quinuclidinyl benzylate is more potent than the (+) isomer (Meyerhoffer 1972) and that esters of 3α-tropanol are more potent than their 3β epimers (Hunt & Robinson 1972). Similar stereochemical effects have also been observed in our laboratory with other tropane derivatives (Niu et al 1990; Gao & Liu 1995; Gao et al 1995a, b, 1996).

To understand better the relationships between chemical structure and pharmacological activity, a series of tropane derivatives was synthesized in our institute (Fig. 1). The purpose was to determine the effects of the structural and stereochemical changes on the pharmacological effects of the tropane series.

In this study we found the tropane ethers, 2α-(2′,2′-diphenyl-2′-hydroxyethoxy) tropane (α-DPT) and its two optical isomers (1*R*,2α*R*-, 1*S*,2α*S*-), were significantly less potent in their anti-muscarinic activity than the tropane ester 2α*R*-tropanyl benzylate, but were equipotent in their anti-nicotinic activity.

Materials and Methods

Drugs

[^{3}H]Quinuclidinyl benzylate (43·3 Ci mmol^{-1}) and [^{3}H]nicotine (78·4 Ci mmol^{-1}) were purchased from Amersham (Bucks, UK). 2α*R*-tropanyl benzylate, 2α-DPT and its two optical isomers were synthesized at our Institute. Hexamethonium, mecamylamine, arecoline, nicotine free base and atropine were from Sigma (St Louis, MO).

Correspondence: Z. G. Gao, Institute of Pharmacology and Toxicology, 27 Taiping Road, Beijing 100850, China.

Arecoline-induced tremor and nicotine-induced convulsions in mice, and the antagonistic effects of the drugs

Experiments were performed on Shanghai mice, 18–22 g, ten in each dose-group. Five doses of each of the drugs to be tested were injected intraperitoneally 15 min before arecoline (8 mg kg^{-1}, s.c.) to estimate the ED50 values of the antagonistic effect of these compounds.

The anti-nicotinic effects of the compounds were evaluated by a procedure similar to that of Niu et al (1990); the tested drugs were injected into the caudal vein 10 min before nicotine free base (0·8 mg kg^{-1}, i.v.) to estimate the antagonistic effects.

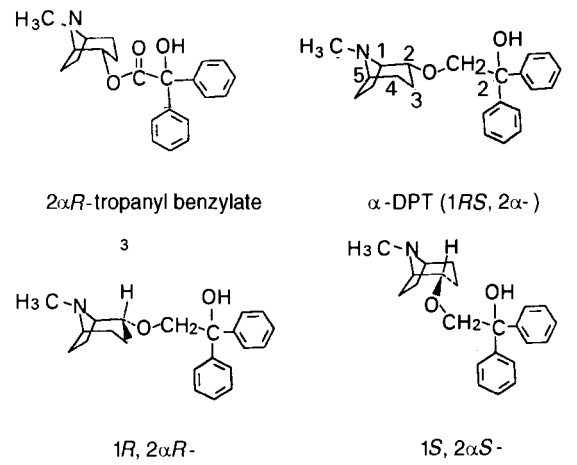

FIG. 1. Structures of 2α*R*-tropanyl benzylate and α-DPT (1*RS*, 2α) and its two optical isomers (1*R*, 2α*R*- and 1*S*, 2α*S*-). The optical purity of the two optical isomers was 100%.

Membrane preparations

Membranes for muscarinic receptor binding were prepared by procedures similar to those previously described (Niu et al 1990). Male or female Wistar rats, 180–220 g, were decapitated. The cerebral cortex was rapidly removed and homogenized in 10 volumes (w/v) of ice-cold 0·32 M sucrose in a glass homogenizer. The whole homogenate was centrifuged at 1000 *g* for 10 min at 4°C. The pellet was discarded and supernatant was re-centrifuged at 20 000 *g* for 30 min at 4°C. The supernatant was decanted and the pellet (P2) was suspended in four volumes of sodium potassium phosphate buffer (50 mM, pH 7·4, 4°C). P2 was then re-homogenized in a glass homogenizer and stored at −20°C. Proteins were determined by the method of Lowry et al (1951) using bovine serum albumin as a standard. Membranes for nicotinic receptor binding were prepared by a procedure similar to that of Zhang & Nordberg (1993).

Binding assay

The binding of various agents to muscarinic receptors was determined by their ability to displace [^{3}H]quinuclidinyl benzylate. Protein (0·1 mg mL^{-1}) was incubated with 0·5 nM [^{3}H]quinuclidinyl benzylate in the presence of tested drugs. Non-specific binding of [^{3}H]quinuclidinyl benzylate was determined in the presence of the unlabelled compound (1·0 mM). Bound [^{3}H]quinuclidinyl benzylate was separated from the unbound ligand by vacuum filtration using Hongguang 49 glass filters (Shanghai, China). The filters were washed three times with ice-cold buffer solution (9 mL). Determinations of binding were performed in duplicate. The filters were then placed in vials containing scintillation liquid (3 mL) containing 2,5-diphenyloxazol (PPO; 0·3%) and 1,4-bis-5-phenyloxazoyl-2-benzene (POPOP; 0·03%) and maintained for over 10 h at room temperature. The radioactivity was assayed by use of an LKB 1215 Rack Beta II liquid scintillation counter at a counting efficiency of 36%. To assay the binding of the compounds to nicotinic receptors, protein (0·2 mg) was incubated with [^{3}H]nicotine (5 nM) in Tris-HCl buffer (pH 8·0; 1 mL) at 4°C for 60 min in the presence of the tested drugs. Non-specific binding of [^{3}H]nicotine was determined in the presence of 10 mM unlabelled nicotine. The samples were then filtered through Hongguang 49 glass filters pre-soaked with 0·5% polyethylenimine solution for 5 h. The remaining procedures were similar to those of the binding assay for muscarinic receptors.

Data analysis

ED50 values of these compounds against arecoline-induced tremor and nicotine-induced convulsion were calculated by the probability–logarithm method (Bliss 1938). Values of equilibrium dissociation constant (K_i) were calculated by the method of Cheng & Prusoff (1973).

Results

Functional studies

As shown in Fig. 2, arecoline-induced tremor in mice can be antagonized by the tropane derivatives. The order of their antagonizing potencies was 2α*R*-tropanyl benzylate > atropine > α-DPT and its isomers. In contrast, the nicotinic receptor antagonist mecamylamine at 2·0 mg kg^{-1} did not prevent arecoline-induced tremor. The ED50 values are summarized in Table 1; there were no significant differences among the ED50 values of α-DPT and its two isomers. 2α*R*-tropanyl benzylate was approximately two orders of magnitude more potent than the tropane ethers.

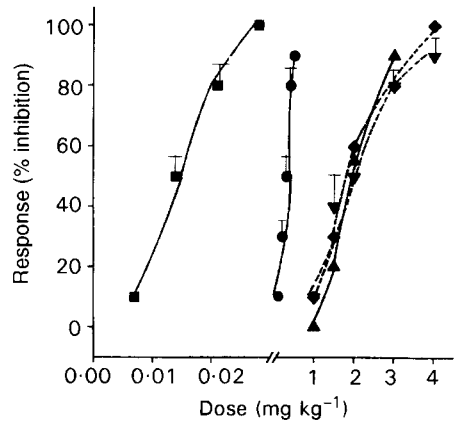

FIG. 2. Dose–response curves for 2α-*R*-tropanyl benzylate (■), α-DPT (▲) and its isomers 1*R*, 2α*R*- (▼) and 1*S*, 2α*S*- (◆), and atropine (●) on arecoline-induced tremor. Different doses of antagonists were injected intraperitoneally 15 min before arecoline (8 mg kg^{-1}, s.c.). Mean ± s.d. There were ten mice in each dose-group.

Fig. 3 shows that nicotine-induced convulsions in mice could be prevented by 2α*R*-tropanyl benzylate and by α-DPT and its isomers. Mecamylamine also showed potent anti-nicotinic effects. In contrast, atropine had very weak anti-nicotinic activity (Table 1). There were no significant differences in ED50 values of 2α*R*-tropanyl benzylate, α-DPT and its isomers for prevention of nicotine-induced convulsion (Table 1).

Binding profiles of the tropane derivatives to central muscarinic receptors

As shown in Fig. 4, the binding of [^{3}H]quinuclidinyl benzylate to rat-brain muscarinic receptors was inhibited by 2α*R*-tropanyl benzylate and by α-DPT and its isomers. A classic muscarinic antagonist, atropine, was also potent in displacing specific binding of [^{3}H]quinuclidinyl benzylate, but other non-muscarinic agents, such as hexamethonium, mecamylamine and nicotine, even at concentrations as high as 10 mM, displaced less than 15% of the specific binding of [^{3}H]quinuclidinyl benzylate (data not shown). The results showed that muscarinic receptors had similar affinities to α-DPT and its two isomers. α-DPT and its two isomers were about three orders of magnitude less potent than 2α*R*-tropanyl benzylate. The K_i values are summarized in Table 1. The order of potencies of the tested drugs to displace [^{3}H]quinuclidinyl benzylate was 2α*R*-tropanyl benzylate > atropine > tropane ethers.

Effects of tropane derivatives on [^{3}H]nicotine binding

To determine the binding specificity of these compounds, experiments were performed with [^{3}H]nicotine. The tropane derivatives and the classical nicotinic receptor antagonist, mecamylamine, at concentrations (10 μM) which produced more than 80% inhibition of [^{3}H]quinuclidinyl benzylate binding, had no effect on [^{3}H]nicotine binding to brain membranes.

Table 1. Effects of tropane derivatives on central muscarinic and nicotinic receptors.

	2α-*R*-Tropanyl benzylate	Atropine	α-DPT	1*R*, 2α*R*-	1*S*, 2α*S*-	Mecamylamine
Equilibrium dissociation constant (K_i; nM)	0·027 ± 0·006	2·1 ± 0·43	31·3 ± 4·9	34·9 ± 6·4	36·2 ± 2·7	> 10 000
Concn reducing effect of of arecoline by 50% (ED50; mg kg^{-1})	0·013 ± 0·003	0·26 ± 0·04	1·9 ± 0·27	1·9 ± 0·38	1·8 ± 0·35	Inactive
Concn reducing effect of nicotine by 50% (ED50; mg kg^{-1})	2·3 ± 0·74	> 20	2·3 ± 0·53	2·5 ± 0·62	3·0 ± 0·52	0·1 ± 0·02

The binding of the various agents to muscarinic receptors was determined by their ability to displace [^{3}H]quinuclidinyl benzylate. Protein (0·1 mg mL^{-1}) was incubated with [^{3}H]quinuclidinyl benzylate (0·5 nM) in Na,K phosphate buffer (50 mM; 1 mL) in the presence of the tested drugs. ED50 values were calculated from the LIGAND program and K_i values of the compounds from the Cheng-Prusoff equation (Cheng & Prusoff 1973). Results are expressed as means ± s.e.m., n = 4 for each compound. Five doses of the tested drugs were injected intraperitoneally 15 min before arecoline (8 mg kg^{-1}, s.c.) to estimate the ED50 values of the anti-muscarinic effect of these compounds. Each dose-group comprised 10 Shanghai mice, 18–22 g. For evaluation of the anti-nicotinic effects of the compounds, the tested drugs were injected into the caudal vein 10 min before nicotine (0·8 mg kg^{-1} i.v.).

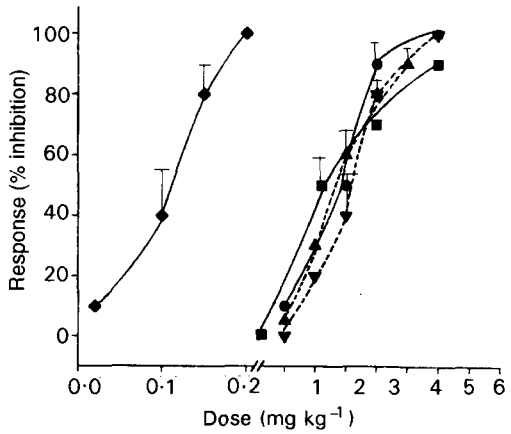

FIG. 3. Dose–response curves for 2α-*R*-tropanyl benzylate (■), α-DPT (●) and its isomers 1*R*, 2α*R*- (▲) and 1*S*, 2α*S*- (▼), and mecamylamine (◆) on nicotine-induced convulsion in mice. Different doses of drugs were injected intravenously 10 min before nicotine (0·8 mg kg^{-1}, i.v.). Mean ± s.d. There were ten mice in each dose-group.

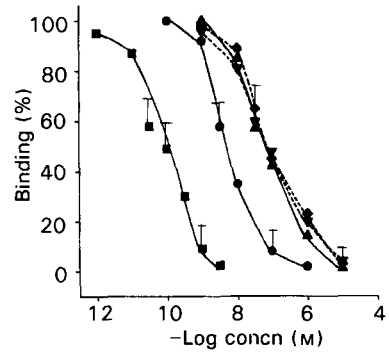

FIG. 4. Competitive binding curves of 2α-tropanyl benzylate (■), atropine (●), α-DPT (▲) and its isomers 1*R*, 2α*R*- (▼) and 1*S*, 2α*S*- (◆) at rat brain muscarinic receptors. Membrane (0·1 mg) of rat cerebral cortex was incubated for 30 min with 0·5 nM [^{3}H]quinuclidinyl benzylate at 35°C in sodium/potassium phosphate buffer (pH 7·4; 50 mM; 1 mL) in the presence of different antagonists. Mean ± s.d. (n = 4).

Discussion

A striking pharmacological difference between 2α*R*-tropanyl benzylate and the tropane ethers was observed in this study. It was demonstrated that the ester group (−O−C=O) is important to the anti-muscarinic activity of 2α*R*-tropanyl benzylate. Replacing the ester group by an ether group (−O−CH_2−), reduced the affinity of 2α*R*-tropanyl benzylate for muscarinic receptors by about three log units. In contrast, the structural change did not affect the anti-nicotinic activity of the compound. Binding assays showed that central muscarinic receptors had no stereoselectivity towards α-DPT and its two enantiomers and the results of functional experiments confirmed this. This result is different from those obtained for 2α-(2′,2′-disubstituted-2′-hydroxyethoxy) tropane (2α-DHET; Gao et al 1995a, b), 2-substituted tropane esters (Atkinson et al 1977), 3-substituted quinuclidinyl ethers (Niu et al 1990) and their optical isomers. Muscarinic receptors had affinities different from those of previously reported compounds and their optical isomers. As the ED50 values of α-DPT and its two isomers in antagonizing nicotine-induced convulsions in mice were not different significantly, it is possible that nicotinic receptors also had no stereoselectivity for the compounds.

It is known that the convulsions produced by nicotine are mediated through nicotinic receptors in brain (Beleslin & Krstic 1986; Martin et al 1989; Abood et al 1993; Gao et al 1995b). This study showed that the affinity of the compounds for nicotinic receptors does not correlate with the findings from functional studies. The difference in the anti-nicotinic activity and the ability to displace the specific binding of [^{3}H]nicotine suggests that these compounds do not act on the recognition site of central nicotinic receptors. As previously reported, other tropane alkaloids and the classical nicotinic receptor antagonists have also been shown to bind with nicotinic receptors with very low affinities, although they showed potent anti-nicotinic activity in-vivo (Martin et al 1989; Banerjee et al 1990; Schmeller et al 1995). Nicotinic receptors are divided into four subtypes: muscle, ganglionic, neuronal CNS and α7 neuronal. Molecular biology studies have elucidated that there are at least ten nicotinic receptor genes in brain: α1, α2, α3, α4, α5, α6, α7 and β2, β3, β4, β5 (Sargent 1993). Of these, α2, α3 and α4 can combine with β2 or β4 subunits to form at least six functional α-bugarotoxin-insensitive nicotinic receptors. Each

of these receptor subtypes has its unique pharmacological properties. The sensitivity of nicotinic receptors to nicotinic receptor antagonists is dependent on the nature of sub-unit composition. As the preparation of the whole cerebral cortex was used in this study, it is not possible to determine which subtypes or subunits were acted upon by the tested drugs.

The mechanisms by which mecamylamine exerts its anti-nicotinic effects have generally been attributed to non-competitive antagonism at nicotinic receptors in the brain (Martin et al 1989). In general, as first reported by Romano & Goldstein (1980), the nicotinic receptor antagonists were rather weak in displacing [^{3}H]nicotine from its binding site. It has been suggested that the low potency of classical nicotinic receptor antagonists such as mecamylamine and hexamethonium in displacing [^{3}H]nicotine binding might be because of the conversion of the binding site into an 'agonist-selective' state (Romano & Goldstein 1980). This is, however, unlikely because antagonists such as dihydro-β-erythroidine and neosurugotoxin show relatively high potency in binding studies (Wonnacott 1990).

It has been suggested that the reason for the low affinity shown by some antagonists might be related to their binding at an allosteric site on the receptor ionophore complex, possibly at a site within the channel rather than at the binding site for nicotine (Wonnacott 1990; Loiacono et al 1993). It is possible that the tropane derivatives also act on the allosteric site of nicotinic receptors.

In summary, this study has demonstrated that 2α*R*-tropanyl benzylate and α-DPT and its optical isomers had both anti-muscarinic and anti-nicotinic activities. The ester group is important for the anti-muscarinic activity of 2α*R*-tropanyl benzylate. The anti-nicotinic activities of these compounds are independent of the structural changes and their anti-muscarinic activities. The tropane derivative exerts its effects on central nicotinic receptors in a manner similar to that of the classical nicotinic receptor antagonist mecamylamine.

References

Abood, L. G., Saraswati, M., Lerner-Marash, N., Hashmi, M. (1993) Affinity ligands and related agents for brain muscarinic and nicotinic cholinergic receptors. Biochem. Pharmacol. 45: 2143–2148

Atkinson, E. R., McRitchie, D. D., Shoer, L. F., Harris, L. S., Archer, S., Aceto, M. A., Pearl, J., Luduena, F. P. (1977) Parasympatholytic (anticholinergic) esters of the isomeric 2-tropanols. 1. Glycolates. J. Med. Chem. 20: 1612–1617

Banerjee, S., Punzi, J. S., Kreilick, K., Abood, L. G. (1990) [^{3}H]Mecamylamine binding to brain membranes, studies with mecamylamine and nicotine analogues. Biochem. Pharmacol. 40: 2105–2110

Beleslin, D. B., Krstic, K. S. (1986) Nicotine-induced convulsions in cats and central nicotinic receptors. Pharmacol. Biochem. Behav. 24: 1509–1511

Bliss, C. I. (1938) The determination of the dosage–mortality curve from small numbers. Quart. J. Pharm. Pharmacol. 11: 192–216

Cheng, Y. C., Prusoff, W. H. (1973) Relationship between the inhibition constant (K_i) and the concentration of inhibitor which causes 50 percent inhibition (I50) of an enzymatic reaction. Biochem. Pharmacol. 22: 3099–3108

Gao, Z. G., Liu, C. G. (1995) Competitive and allosteric binding of 2α-DHET and its optical isomers to rat cardiac muscarinic receptors. Eur. J. Pharmacol. 289: 369–373

Gao, Z. G., Wang, L., Liu, C. G. (1995a) Effects of 2α-DHET and its optical isomers on muscarinic and nicotinic receptors. Life Sci. 56: PL461–466

Gao, Z. G., Wang, L., Liu, C. G., Zhang, Q. K. (1995b) Effects of a new cholinolytic drug of tropanes and its optical isomers on central muscarinic and nicotinic receptors. Pharmacol. Res. 32: 105–109

Gao, Z. G., Wang, L., Liu, C. G. (1996) Allosteric and competitive interactions of 2α-(2′,2′-disubstituted-hydroxyethoxy)tropane and its optical isomers to rat central muscarinic acetylcholine receptors. Life Sciences 58: 2279–2287

Hoyer, D. (1986) Implications of stereoselectivity in radioligand binding studies. Trends Pharmacol. Sci. 7: 227–230

Hunt, R. J., Robinson, J. B. (1972) Analogues and homologues of atropine: anti-acetylcholine activities. J. Pharm. Pharmacol. 24: 324–325

Loiacono, R., Stephenson, J., Stevenson, J., Mitchelson, F. (1993) Multiple binding sites for nicotine receptor antagonists in inhibiting [^{3}H]nicotine binding in rat cortex. Neuropharmacology 32: 847–853

Lowry, O. H., Rosebrough, N. J., Farr, A. L., Randall, R. J. (1951) Protein measurement with the Folin phenol reagent. J. Biol. Chem. 193: 265–275

Martin, B. R., Onaivi, E. S., Martin, J. (1989) What is the nature of mecamylamine's antagonism of the central effects of nicotine. Biochem. Pharmacol. 38: 3391–3397

Meyerhoffer, A. (1972) Absolute configuration of 3-quinuclidinyl benzylate and the behavioral effect in the dog of the optical isomers. J. Med. Chem. 15: 994–995

Niu, W. Z., Zhao, D. L., Liu, C. G. (1990) The effects of a new cholinolytic-8018 and its optical isomers on central muscarinic and nicotinic receptors. Arch. Int. Pharmacodyn. 304: 64–74

Noronha-blob, L., Kachur, J. F. (1991) Enantiomers of oxybutynin: in-vitro pharmacological characterization at M1, M2 and M3 muscarinic receptors and in-vivo effects on urinary bladder contraction, mydriasis and salivary secretion in guinea-pigs. J. Pharmacol. Exp. Ther. 256: 562–567

Romano, C., Goldstein, A. (1980) Stereospecific nicotine receptor on rat brain membranes. Science 210: 647–650

Sargent, P. B. (1993) The diversity of neuronal nicotinic acetylcholine receptors. Annu. Rev. Neurosci. 16: 403–443

Schmeller, T., Sporer, F., Sauerwein, M., Wink, M. (1995) Binding of tropane alkaloids to nicotinic and muscarinic acetylcholine receptors. Pharmazie 50: 493–495

Waelbroeck, M., Tastenoy, M., Camus, J., Feifel, R., Mutschler, E., Strohman, C., Tacke, R., Lambrecht, G., Christophe, J. (1989) Stereoselectivity of the interaction of muscarinic antagonists with their receptors. Trends Pharmacol. Sci. 10 (Suppl.): 65–69

Wonnacott, S. (1990) Characterization of nicotine receptor sites in the brain. In: Wonnacott, S., Russel, M. A. H., Stolerman, I. P. (eds) Nicotine Psychopharmacology. Oxford University Press, Oxford, pp 226–277

Zhang, X., Nordberg, A. (1993) The competition of (−)-[^{3}H]nicotine binding by the enantiomers of nicotine, nornicotine and anatoxin-a in membranes and solubilized preparations of different brain regions of rat. Naunyn Schmiedebergs Arch. Pharmacol. 348: 28–34